CLIQ Protection Design for the Graded Nb_3Sn Research Racetrack Dipole Demonstrator (R2D2)

Dong Liu, *Member, IEEE*, Tiina Salmi, *Member, IEEE*, Valerio Calvelli, and Etienne Rochepault

***Abstract*—The Research Racetrack Dipole Demonstrator (R2D2) is being studied as a demonstrating magnet for future FCC magnets. The R2D2 is meant to prove the feasibility of grading in block-coil Nb_3Sn dipoles and explore quench behaviors at a very high current. This short model provides an opportunity to study quench protection concepts which will be needed for the full-scale FCC magnets. Both quench heaters and CLIQ (coupling loss induced quench) are under study. This paper presents the research work on the CLIQ protection. The work includes CLIQ design methods and configurations, and comparative studies of various CLIQ configurations for maximizing the CLIQ effectiveness. The results show that the most effective CLIQ configuration is able to quench 80% of the coil turns at the nominal current within 3 ms, leaving 20 ms for detection and validation time while keeping the maximum hotspot temperature within 350 K. The study shows that protection of R2D2 using only CLIQ may be feasible under certain assumptions.**

***Index Terms*—Accelerator magnet, CLIQ, FCC, Nb_3Sn, R2D2, quench protection.**

I. Introduction

THE magnet named Research Racetrack Dipole Demonstrator (R2D2) is being studied within the collaboration between CEA and CERN as an intermediate step towards the FCC Flared-end Dipole Demonstrator (F2D2) [1], [2], [3]. R2D2 is simplified from F2D2 but designed to maintain the key challenges foreseen in F2D2. The goal of R2D2 is to prove the grading in coils with Nb_3Sn Rutherford cables representative of FCC and to explore quench behaviors at a very high current. CEA is collaborating with Tampere University to validate quench protection technologies.

R2D2 is a dipole magnet designed for operation at 4.2 K. R2D2 is made of two single-layer nested sub-coils: the high field (HF) and the low field (LF) coils, as illustrated in and Fig. 1 [4]. Its full length is 1.4 m. Such short magnets are usually protected with external dump resistors [5], [6]. For longer magnets, in addition to energy extraction, the protection is usually designed with quench heaters alone or combination of quench heaters and CLIQ [7], [8], [9]. We studied the protection methods to see if the R2D2 could be protected with only quench heaters [10]. This paper only presents the CLIQ protection research work. The first part is to describe the CLIQ design methods and configurations for R2D2 for maximizing the CLIQ effectiveness. The second part is comparative studies and assessment of four CLIQ configurations.

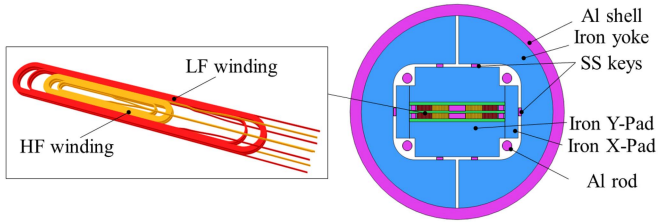

Fig. 1. R2D2 magnet model. Left: zoom-in HF and LF windings. Right: cross-sectional view. The overall radius (Al shell) is 242 mm.

TABLE I
Main Parameters of the R2D2 Magnet

Parameter	Value	Parameter	Value
Nominal current (A)	14588	Superconductor	Nb_3Sn
Straight part length (mm)	566.2	RRR HF cable	200
Overall length (mm)	1400	RRR LF cable	450
Equivalent 2D length (mm)	835	Temperature (K)	4.2
Inductance (mH)	4.921	Energy density (kJ/kg)	17.457
Copper/SC ratio HF	0.9	Copper/SC ratio LF	1.8
No. of strands HF	21	No. of strands LF	34
No. of turns HF	16	No. of turns LF	21
$J_c(16\ \mathrm{T}, 4.2\ \mathrm{K})$ HF (A/mm^2)	1500	$J_c(16\ \mathrm{T}, 4.2\ \mathrm{K})$ LF (A/mm^2)	1200

II. The R2D2 Magnet

The magnet has four blocks and each pole has two blocks. One block (HF1 or HF2) is with the high field Nb_3Sn cables, and the other block (LF1 or LF2) is with the low field Nb_3Sn cables. The important magnet and cable parameters are summarized in Table I. The equivalent 2D length in Table I is obtained by integrating the magnetic flux density along the magnet axis and then dividing it by the magnetic flux density at the magnet center. The other parameters, such as cable dimensions, can

Manuscript received 13 November 2022; revised 5 February 2023 and 11 February 2023; accepted 11 February 2023. Date of publication 22 February 2023; date of current version 7 March 2023. This work was supported by the Academy of Finland Project (HiQuench) under Grant 336287. *(Corresponding author: Dong Liu.)*

Dong Liu was with the Unit of Electrical Engineering, Tampere University, FI-33720 Tampere, Finland. He is now with the School of Energy Systems, LUT University, FI-15210 Lahti, Finland (e-mail: dong.liu@lut.fi).

Tiina Salmi is with the Unit of Electrical Enginerring, Tampere University, FI-33720 Tampere, Finland.

Valerio Calvelli and Etienne Rochepault are with IRFU, CEA, Université Paris-Saclay, Paris F-91191, France.

Color versions of one or more figures in this article are available at https://doi.org/10.1109/TASC.2023.3247983.

Digital Object Identifier 10.1109/TASC.2023.3247983

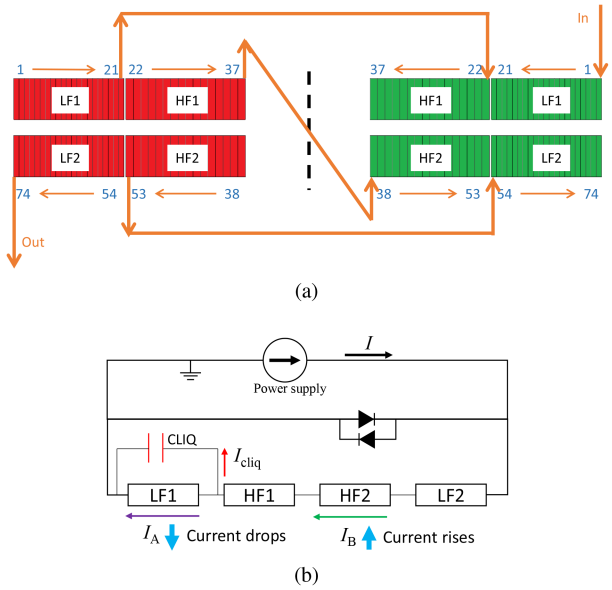

Fig. 2. Connection of turns and blocks of the R2D2 magnet: (a) electrical order of turns, (b) series connection of blocks.

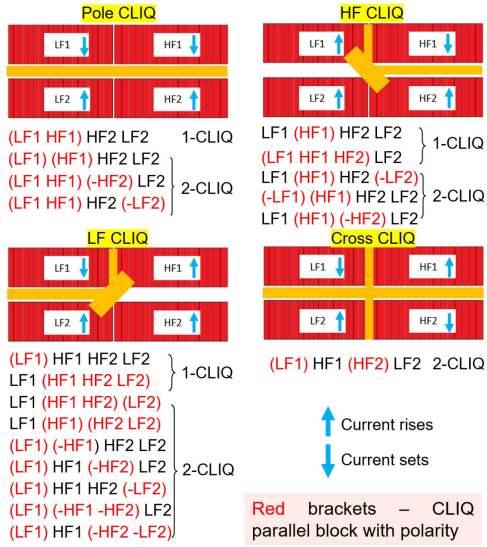

Fig. 3. CLIQ configurations to form the boundaries that potentially maximizes the CLIQ effectiveness. (Orange strips: targeted CLIQ energy distribution) .

refer to [1]. The connection of the turns and blocks, as shown in Fig. 2(a) and (b), respectively, has been determined by CEA. The electrical order of the turns determines the possibilities of CLIQ configurations for the magnet. For example, LF1 and LF2 cannot have the same single CLIQ circuit since they are not adjacent to each other. They must have separate CLIQ circuits if two CLIQs can be used. HF1 and HF2 can have the same single CLIQ circuit since they are adjacent.

III. CLIQ Design Method and Configurations

CLIQ energy is deposited at the boundary between blocks where the current of one side is rising and the current of the other side is decreasing. If we use the convention of current direction for the CLIQ and magnet circuits as shown in Fig. 2(b), we can derive and build CLIQ configurations for maximizing the CLIQ effectiveness according to the CLIQ theory in [11], [12], [13], [14]. For the R2D2 magnet, as shown in Fig. 3, such boundaries can occur between the two poles (Pole CLIQ), around one HF block (HF CLIQ), around one LF block (LF CLIQ), or between the four blocks like a cross-shape distribution (Cross CLIQ). The CLIQ energy should be deposited at such boundaries. The CLIQ configurations for each of these CLIQ energy deposition patterns are summarized in Fig. 3. Only 1-CLIQ and 2-CLIQ configurations are given here. The red block names in red brackets mean which blocks are connected with a CLIQ circuit in parallel. The minus sign means the CLIQ voltage direction is reversed.

We used STEAM-LEDET to model and calculate the R2D2 magnet and its CLIQ protection performance [15]. An equivalent length of 0.835 m is used instead of the full length or the straight part length. However, LEDET cannot model unsymmetrical CLIQ configurations. This means multiple CLIQs cannot be modeled unless their parameters are identical, such as voltage, capacitance and lead resistance. This limitation reduced the number of CLIQ configurations in this study, especially those with a negative CLIQ voltage. However, it is not necessary to look at all the possible CLIQ configurations. We started from the simplest and most representative CLIQ configurations with one CLIQ, i.e., Pole CLIQ, HF CLIQ, LF CLIQ. We also studied the Cross CLIQ although it required two CLIQs due to the block connection. Their CLIQ configurations are given in Fig. 3. The results are enough to reveal how CLIQ protection performs for R2D2.

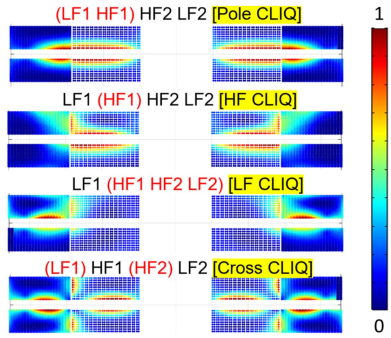

Fig. 4. CLIQ energy distribution obtained from LEDET calculations, normalized to the maximum value when the energy reaches its peak after the CLIQ is triggered.

We applied LEDET to calculate the CLIQ energy distribution. As shown in Fig. 4, the CLIQ energy distribution meets what we have expected from the correlation between current changes that form boundaries and CLIQ energy deposition patterns. The Pole CLIQ deposits energy at the boundaries between the poles. The HF and LF CLIQs deposit energy around the HF1 block and the LF1 block, respectively. The Cross CLIQ deposits energy between the four blocks.

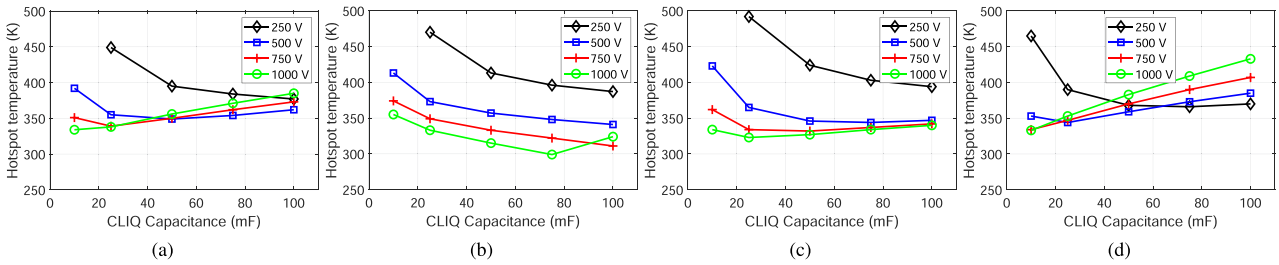

Fig. 5. Parameter sweep of the CLIQ configuration optimization. (a) Pole CLIQ, (b) HF CLIQ, (c) LF CLIQ, (d) Cross CLIQ.

TABLE II
PARAMETERS AND PERFORMANCE OF OPTIMIZED CLIQ CONFIGURATIONS

	Pole CLIQ	HF CLIQ	LF CLIQ	Cross CLIQ
Voltage U_C (V)	995	1000	994	1000
Capacitance (mF)	10	75	25	10
Hotspot temperature (K)	334	299	323	333
Max. voltage to ground (V)	1000	780	1000	720

IV. Optimization of CLIQ Configurations

The four CLIQ configurations were optimized before they went to be compared and analyzed. The CLIQ voltage and capacitance were chosen as the optimization variables. The objective of the optimization was the adiabatic hotspot temperature. As a constraint, the maximum voltage to ground of the magnet should be no higher than 1000 V. The detection time was assumed to be 15 ms. This detection time consists of the times for both detection and validation, meaning the total time for detecting a local hotspot and validating it. In the LEDET model and calculation, the detection time means the current stays at the nominal value (14588 A) for 15 ms before the CLIQ is triggered. We applied LEDET to calculate the CLIQ performance and extracted the data of hotspot temperatures and maximum voltages to ground of each CLIQ configuration.

The maximum voltage to ground occurs at the beginning of the CLIQ triggering. It is roughly proportional to the CLIQ voltage, but the proportion ratio is different from configuration to configuration. For the Pole CLIQ and LF CLIQ configurations, the maximum voltage to ground is slightly higher than the CLIQ voltage. The difference is a few volts. With the HF CLIQ and Cross CLIQ configurations, the maximum voltage to ground is lower than the CLIQ voltage. The voltages to ground are 0.78 and 0.72 of U_C with HF CLIQ and Cross CLIQ, respectively.

The hotspot temperatures with respect to the CLIQ voltage and capacitance are shown in Fig. 5 for the four CLIQ configurations. The lowest hotspot temperatures are found for each configuration and summarized in Table II. The HF CLIQ gives the lowest hotspot temperature being 299 K. The other three configurations give similar hotspot temperatures between 320 K and 340 K. The Pole CLIQ and LF CLIQ have their lowest hotspot temperatures with the CLIQ voltage being 1000 V, leading to the voltage to ground being slightly over 1000 V. Thus, the CLIQ voltage should be a bit lower than 1000 V instead for limiting the voltage to ground.

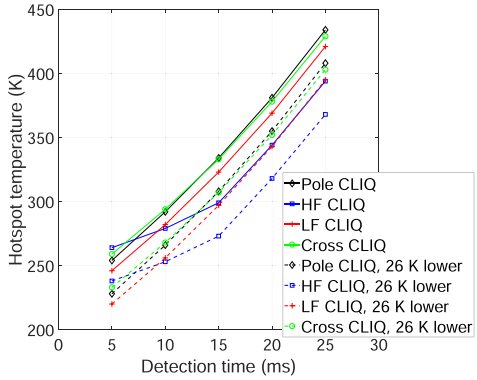

Fig. 6. Effects of detection time on adiabatic hotspot temperature calculated with LEDET. Effects of subtracting 26 K from the LEDET result are shown in the dashed curves.

V. Comparison and Analysis of CLIQ Configurations

A. *Effects of Detection Time on the Hotspot Temperature*

In the optimization, we assumed the detection time to be 15 ms. With this assumption, the hotspot temperature after optimization was always below 350 K. By imposing an upper limit of 350 K to the hotspot temperature, we studied the corresponding limit for the detection time, thereby indicating how fast the quench detection must be. We swept the detection time from 5 ms to 25 ms and the hotspot temperature of the four CLIQ configurations was calculated with LEDET. Each configuration has its optimum CLIQ voltage and capacitance.

The curves are shown in Fig. 6. The Pole CLIQ, LF CLIQ and Cross CLIQ have similar trends with an increasing detection time. The HF CLIQ has lower hotspot temperatures. The required detection time for limiting the hotspot temperature below 350 K is 16.7 ms (Pole CLIQ), 20.6 ms (HF CLIQ), 17.9 ms (LF CLIQ) and 16.9 ms (Cross CLIQ).

We used two other tools Coodi [16] and STEAM-SIGMA [18] to crosscheck the LEDET calculation for the R2D2 magnet. In the crosschecking model, all the turns of the magnet are quenched after 15-ms constant nominal current operation. The

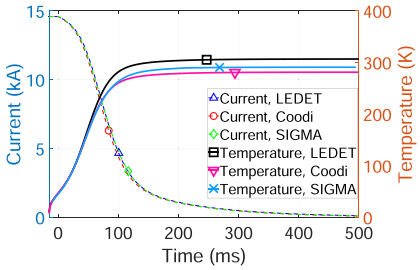

Fig. 7. Crosscheck of magnet current and hotspot temperature between LEDET, Coodi and SIGMA. A discharge model of the R2D2 magnet is used.

CLIQ is not triggered so the current decays only due to the resistance of the magnet cables in the normal state. The magnet current and hotspot temperature from LEDET, Coodi and SIGMA calculations are plotted in Fig. 7. The curves of current agree well, and only tiny discrepancies are seen. LEDET simulated the highest hotspot temperature which is 26 K higher than the lowest from Coodi. The temperature discrepancies of the three tools are caused by the slight disagreements of the current and the differences of material properties used in the three tools. Unfortunately, the material properties could not be made identical between the tools. Therefore, LEDET can be considered conservative, and the 26 K difference could be regarded as a safety margin. As shown in the dashed curves of Fig. 6, we investigated the effect of the hotspot temperatures, 26 K lower than the LEDET-calculated numbers, on the detection time. Then the required detection time for limiting the hotspot temperature below 350 K becomes 19.5 ms (Pole CLIQ), 23.3 ms (HF CLIQ), 20.7 ms (LF CLIQ) and 20.0 ms (Cross CLIQ).

B. Magnet Currents

From the hotspot temperature point of view, the HF CLIQ configuration seems to outperform the other three configurations. If we look at the current waveforms (calculated from LEDET) in Fig. 8, however, the HF CLIQ configuration leads to 2.4 times the nominal current in the HF windings. The current may be too high. The current oscillation in the LF winding is quite weak compared to that of the HF winding and that of the other three configurations. Note that the maximum hotspot temperature occurs in the LF windings. This weak oscillation explains why the HF CLIQ configuration results in such low hotspot temperatures. The overshoot of magnet current of the HF CLIQ configuration may not be acceptable. Thus, we did not consider it for the next study anymore.

C. Time to Quench the Magnet

The CLIQ effectiveness was thought to determine the speed of quenching the magnet. We calculated the time to quench 80% and 100% of the turns, respectively. The results are shown in Fig. 9 when the remaining three CLIQ configurations (HF CLIQ is left out) are compared under the same CLIQ parameters. With the lower CLIQ voltage (500 V) and capacitance (25 mF), quenching most turns is fastest by the Cross CLIQ. Using a larger capacitance (50 mF) significantly shortens the time with the Pole

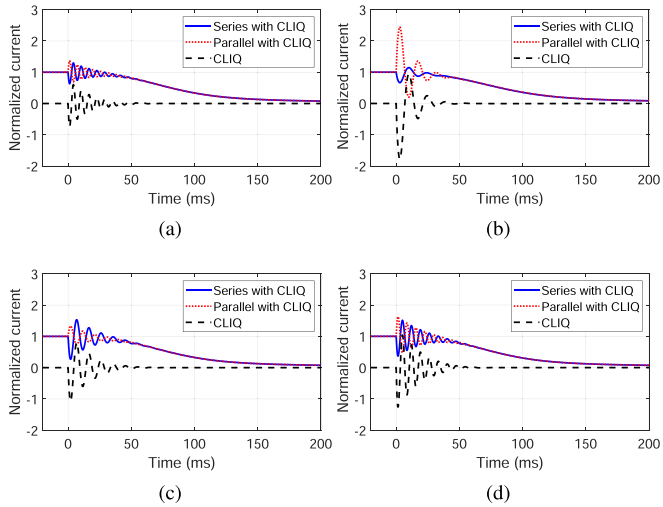

Fig. 8. Magnet and CLIQ currents normalized to the nominal current (14588 A). (a) Pole CLIQ, (b) HF CLIQ, (c) LF CLIQ, (d) Cross CLIQ.

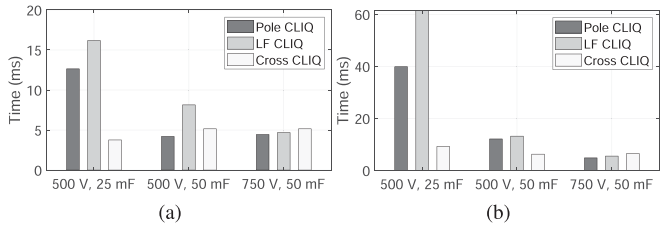

Fig. 9. Time to quench the magnet under the same CLIQ parameters. (a) 80% turns quenched, (b) 100% turns quenched.

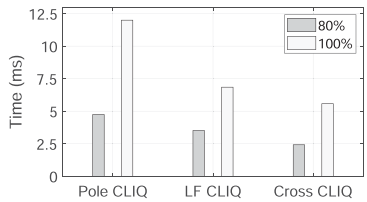

Fig. 10. Time to quench the magnet. The CLIQ configurations are with their optimized voltage and capacitance.

CLIQ while the quench time of the LF CLIQ is still the longest. With the higher CLIQ voltage (750 V), the LF CLIQ becomes faster than the Cross CLIQ while the Pole CLIQ becomes the fastest. This result meets the expectation from the CLIQ energy distribution in Fig. 4. The Pole CLIQ's CLIQ energy covers the most turns as compared to the other configurations. However, the Pole CLIQ is not always the fastest and the CLIQ parameters can make differences.

The time to quench the magnet is also compared when the CLIQ configurations use their optimum voltage and capacitance (see Table II). The result is shown in Fig. 10. The optimized Cross CLIQ configuration becomes the fastest. It is worth noting that the longest time (the Pole CLIQ) remains shorter than 12 ms, which is considered very fast.

VI. Conclusion

The CLIQ design method for the R2D2 magnet was presented for maximizing the CLIQ effectiveness based on the magnet features. The R2D2 magnet model with CLIQ protection was built with STEAM-LEDET. Four CLIQ configurations (Pole CLIQ, HF CLIQ, LF CLIQ and Cross CLIQ) for protecting R2D2 were optimized for the lowest adiabatic hotspot temperature.

The required detection time of the studied CLIQ configurations was found for limiting the hotspot temperature below 350 K. The HF CLIQ allows for the longest detection time (20.6 ms to 23.3 ms). However, the HF CLIQ leads to excessive magnet currents (2.4 times nominal) and is thus not considered anymore.

The time to quench 80% and 100% turns of the magnet is used to assess the effectiveness of the CLIQ configurations. The Pole CLIQ, LF CLIQ and Cross CLIQ are able to quench 80% of turns within 2 to 5 ms, and quenching 100% of turns takes 5 to 12 ms. The optimized Cross CLIQ is considered as the fast configuration since it is able to quench 80% of the coil turns with the nominal current within 3 ms, leaving 20 ms for detection and validation time while keeping the maximum hotspot temperature within 350 K. The Pole CLIQ and LF CLIQ give both similar hotspot temperatures and needed detection times, and their advantage is that they need only one CLIQ unit. All these options could still be considered in the future analysis.

During the benchmark crosscheck between LEDET, Coodi and SIGMA, LEDET simulated the highest hotspot temperature, with a difference of 26 K from the minimum value. The LEDET results are used as conservative estimates. Considering a margin of 26 K would provide an additional 2 to 3 ms in the required detection time.

The study was done only at the high nominal current. In real quench protection design, one should check if the CLIQ power is enough to quench the magnet also at other current levels. This must be done in future before we fully conclude the suitability of different CLIQ configurations.

The study shows that protection of R2D2 using only CLIQ may be feasible under aggressive assumptions (relatively short detection time and in one particular configuration). An alternative using quench heaters has also been studied separately. As a demonstrator, the R2D2 magnet will be protected safely using a dump resistor. CLIQ and quench heaters will be used for quench protection studies.

Acknowledgment

We thank E. Ravaioli and M. Wozniak from CERN for helping us use STEAM-LEDET and STEAM-SIGMA.

References

[1] V. Calvelli et al., "R2D2, the CEA graded Nb_3Sn research racetrack dipole demonstrator magnet," *IEEE Trans. Appl. Supercond.*, vol. 31, no. 5, Aug. 2021, Art. no. 4002706.

[2] H. Felice et al., "F2D2: A block-coil short-model dipole toward FCC," *IEEE Trans. Appl. Supercond.*, vol. 29, no. 5, Aug. 2019, Art. no. 4001807.

[3] E. Rochepault et al., "3D conceptual design of F2D2, the FCC block-coil short model dipole," *IEEE Trans. Appl. Supercond.*, vol. 30, no. 4, Jun. 2020, Art. no. 4001005.

[4] E. Rochepault et al., "3D conceptual design of R2D2, the research racetrack dipole demonstrator," *IEEE Trans. Appl. Supercond.*, vol. 32, no. 6, Sep. 2022, Art no. 4004605.

[5] L. Coull, D. Hagedorn, V. Remondino, and F. Rodriguez-Mateos, "LHC magnet quench protection system," *IEEE Trans. Magn.*, vol. 30, no. 4, pp. 1742–1745, Jul. 1994.

[6] K. Wang et al., "Updates on fast discharge resistor system for comprehensive research facility for fusion technology," *Fusion Eng. Des.*, vol. 172, 2021, Art. no. 112781.

[7] T. Salmi et al., "Suitability of different quench protection methods for a 16 T block-type Nb_3Sn accelerator dipole magnet," *IEEE Trans. Appl. Supercond.*, vol. 27, no. 4, Jun. 2017, Art. no. 4702305.

[8] M. Prioli et al., "The CLIQ quench protection system applied to the 16 T FCC-hh dipole magnets," *IEEE Trans. Appl. Supercond.*, vol. 29, no. 8, Dec. 2019, Art. no. 4703209.

[9] J. Ferradas Troitino et al., "On the mechanical behavior of a Nb_3Sn superconducting coil during a quench: Two-dimensional finite element analysis of a quench heater protected magnet," *Cryogenics*, vol. 106, 2020, Art. no. 103054.

[10] T. Salmi, D. Liu, V. Calvelli, and E. Rochepault, "Quench protection on Nb3Sn high field magnets using heaters, a strategy applied to the graded race-track dipole R2D2," *IEEE Trans. Appl. Supercond*, 2023.

[11] E. Ravaioli, "CLIQ a new quench protection technology for superconducting magnets," Ph.D. dissertation, University of Twente, The Netherlands, 2015.

[12] E. Ravaioli et al., "Quench protection system optimization for the high luminosity LHC Nb_3Sn quadrupoles," *IEEE Trans. Appl. Supercond.*, vol. 27, no. 4, Jun. 2017, Art. no. 4702107.

[13] E. Ravaioli et al., "Quench protection of the first 4-m-long prototype of the HL-LHC Nb_3Sn quadrupole magnet," *IEEE Trans. Appl. Supercond.*, vol. 29, no. 5, Aug. 2019, Art. no. 4701405.

[14] E. Ravaioli, V. I. Datskov, G. Kirby, M. Maciejewski, H. H. J. ten Kate, and A. P. Verweij, "CLIQ-based quench protection of a chain of high-field superconducting magnets," *IEEE Trans. Appl. Supercond.*, vol. 26, no. 4, Jun. 2016, Art. no. 4000305.

[15] E. Ravaioli et al., "Lumped-element dynamic electro-thermal model of a superconducting magnet," *Cryogenics*, vol. 80, no. 3, pp. 346–356, Dec. 2016.

[16] T. Salmi et al., "Quench protection analysis integrated in the design of dipoles for the future circular collider," *Phys. Rev. Accelerators Beams*, vol. 20, no. 3, 2017, Art. no. 032401.

[17] T. Salmi, T. Tarhasaari, and S. Izquierdo-Bermudez, "A database for storing magnet parameters and analysis of quench test results in HL-LHC Nb_3Sn short model magnets," *IEEE Trans. Appl. Supercond.*, vol. 30, no. 4, Jun. 2020, Art no. 4703705.

[18] "STEAM website," Accessed Feb. 11, 2023. [Online]. Available: https://espace.cern.ch/steam/_layouts/15/start.aspx#/SIGMA/